Electronic impurity-scattering anisotropy in *Cu*Al

A. J. Baratta
Pennsylvania State University, University Park, Pennsylvania 16802

A. C. Ehrlich
Naval Research Laboratory, Washington, D.C. 20375

(Received 24 March 1981)

Magnetic-field-induced surface-state resonances in the (110) sample plane of dilute *Cu*Al alloy were used to study the electron—impurity-scattering rate. Twenty-six locations on the Fermi surface of Cu were measured. By carefully considering the line shapes and linewidths of the surface-state resonances, electron—impurity-scattering rates were determined for both pure Cu and a dilute *Cu*Al alloy. Analysis of the change in scattering rate upon alloying shows that the aluminum-induced scattering varies by more than a factor of 3 over the Fermi surface. The largest change in scattering rate occurs near the Brillouin zone boundaries, [111] and [100] directions. The variation of the scattering rate follows closely the variation in the *p*-wave component of the Cu electron wave function. Based on this variation and the known band structure of Cu, the authors conclude that the scattering potential introduced in Cu by Al connects primarily the *p* states.

I. INTRODUCTION

Magnetic-field-induced surface-state resonances[1–4] have provided a unique and powerful experimental technique for the investigation of anisotropic thermal scattering of electrons in pure metals.[5,6] Magnetic-field-induced surface-state resonance studies are ideally suited for anisotropic electron scattering rate measurements since the electron states contributing to the resonance lines are confined to small regions of the Fermi surface. In this paper we report on the first investigation of anisotropic impurity scattering of electrons as measured by magnetic-field-induced surface states. In particular, electron scattering due to Al was investigated in the (110) sample plane of Cu. It will be shown that the electron scattering rate is highly anisotropic and that the anisotropy is principally determined by the *p*-state character of the copper electron wave function.

In the next two sections we describe how magnetic-field-induced surface-state resonances can be used to determine scattering rates and how the experiment was conducted and the results obtained. In the final section, the electron—impurity-scattering rates and the implications to be drawn are discussed. The variation of the scattering rate over the Fermi surface is seen to be related to the variation of the *p*-like character of the Cu electron wave function.

II. METHOD

In the presence of a weak magnetic field parallel to the sample surface, electrons near the surface of a

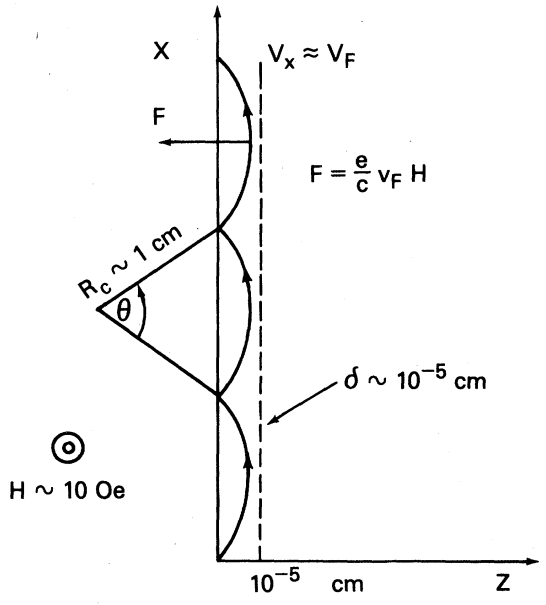

FIG. 1. Schematic representation of surface states showing electron skipping trajectory induced by applied magnetic field, H. R_c is the radius of curvature of the electron orbit, v_F the Fermi velocity, δ the skin depth. θ is typically 1—2 degrees.

metal are trapped in quantum-mechanical bound surface states.[1,2] Classically, the electrons may be viewed as moving along the surface with a periodic skipping motion (Fig. 1). Transition between these surface states may be observed by measurement of the change in the microwave surface impedance of the metal with applied magnetic field. The resonant magnetic field is given by[2]

$$H_{mn} = \frac{\hbar}{e}\left[\frac{\omega}{a_n - a_m}\right]^{3/2}\left[\frac{2K}{v_F^3}\right]_{\perp}^{1/2}, \tag{1}$$

where ω is the microwave frequency, a_m is the zeros of the Airy functions[7] [$\mathrm{Ai}(a_m) = 0$, $m = 1,2$, etc., where Ai is the Airy function], K the local radius of curvature of the Fermi surface, and v_F the Fermi velocity. The symbol $\perp$ denotes the component of the Fermi velocity and projection of the Fermi-surface radius of curvature in the plane perpendicular to the applied magnetic field direction.

The region of the Fermi surface from which the resonance signals originate is determined by those points for which the resonance parameter $(K/v_F^3)_{\perp}^{1/2}$ has local extrema.[8] The regions for which the resonance parameter takes on extremal values are determined by the Fermi-surface geometry, Fermi velocity, and magnetic field orientation. It is possible for more than one region of the Fermi surface to give rise to a signal for a given magnetic field orientation. Typically, the regions are from 3° to 10° in length and 1°—2° in width with respect to the center of the Brillouin zone.[5] One thus obtains very localized values for the various parameters associated with surface-state resonances. The values obtained are weighted averages over the small regions.[5]

In the actual experiment, one does not measure the surface impedance Z but instead the real part of the derivative of the surface impedance taken with respect to the applied magnetic field H, dR/dH. The peaks in the derivative of the real part of the surface impedance with respect to the magnetic field dR/dH occur near the resonant field values given by (1) above.

The shape of the resonance spectrum is given to a good approximation by[1,2]

$$\mathrm{Re}\left[\frac{dZ}{dH}\right] = \mathrm{Re}\left[\text{const}\times(i-\sqrt{3})\frac{d}{dH}\int dk_y\left[v_x(k_y)\sum_{mn}\frac{\alpha_{mn}^2(k_y,H,\delta)}{\omega-\omega_{mn}(H,k_y)+i\Gamma(k_y,H)}\right]\right], \tag{2}$$

where k_y is the $\vec{k}$-space coordinate along the magnetic field. The quantity α_{mn} is the matrix element between the surface-state wave functions ϕ_m and ϕ_n and the electric field in the anomalous-skin-effect skin depth δ of the metal. The wave functions may be shown to be Airy functions.[1,2] The rf current is taken to be in the x direction. The quantity v_x is the component of the Fermi velocity along the rf field. The quantity ω_{mn} is the difference in energy between surface states divided by $\hbar$. The dispersive term $i\Gamma$ accounts for electron scattering.

To carry out numerical evaluation of the expression for the resonance spectrum in (2) above, Jensen[9] suggests that the relationship be expressed in terms of a suitably normalized magnetic field coordinate h defined by

$$h = \frac{e}{\hbar}(v_x^3/2K\omega^3)^{1/2}H = \gamma H, \tag{3}$$

such that the resonance expression in terms of the normalized field is given by

$$h_{mn} = (\zeta_m - \zeta_n)^{-3/2}. \tag{4}$$

According to Nee *et al.*,[2] the matrix elements α_{mn} are functions of H and the skin depth δ. If one defined an effective skin depth β given by

$$\beta = (v_x/2K\omega)^{1/2}(1/\delta), \tag{5}$$

then the matrix element may be written as a function of h and β. Interchanging the differentiation d/dH with the k_y integration and expressing the derivative in terms of the normalized field, one obtains the resonance spectrum as

$$\frac{dZ}{dH} = \text{const}\times\int dk_y v_x\gamma\frac{d}{dh}\sum_{mn}(i-\sqrt{3})\frac{\alpha_{m,n}^2(\beta,h)}{1-h^{2/3}(\zeta_m-\zeta_n)+i\Gamma/\omega}. \tag{6}$$

The quantities h, v_x, γ, and β are functions of k_y.

The expression inside the integral may be shown to be the resonance spectrum of a cylindrical Fermi surface.[1] It is a function of β and Γ only. If one now approximates the integration by a finite sum, one obtains

$$\frac{dZ}{dH} = \text{const} \times \sum_j \Delta k_{yj} v_x(k_{yj}) \gamma(k_{yj}) \frac{d}{dh}(i - \sqrt{3}) \sum_{mn} \frac{\alpha_{mn}^2(\beta,h)}{1 - h^{2/3}(\zeta_m - \zeta_n) + i\Gamma/\omega} . \quad (7)$$

This approximation is equivalent to reconstructing an arbitrary Fermi surface by a series of concentric cylinders of differing radii having axes parallel to the magnetic field. The process allows one to obtain a series of library spectra which may be scaled according to the expression for the normalized field [Eq. (3) above]. Such a technique allows for computer generation of an arbitrary spectrum from the library spectra.

The shape of the resonance spectrum is related to the electronic scattering rates through the dependence on Γ. For example, in Cu, Doezema[5] has shown that the relative half-width $\Delta H/H$ of the resonant peak corresponding to the transition from the $n = 1$ to the $m = 2$ surface states is given by

$$\frac{\Delta H}{H} = 0.02 + 1.56\Gamma^* . \quad (8)$$

The quantity Γ^* is the total scattering rate Γ, for the electrons under consideration, divided by ω the microwave frequency. The scattering rate may be written as the sum of the thermal scattering, impurity scattering, and surface scattering rates:

$$\Gamma(k) = \Gamma_{\text{thermal}} + \Gamma_{\text{impurity}} + \Gamma_{\text{surface}} . \quad (9)$$

The impurity term is taken as $1/\tau$, the reciprocal of the relaxation time due to bulk scattering events. If the scattering is anisotropic, then the relaxation time will be a function of k. By measurement of the surface-state resonance spectrum in the pure metal and in an alloy, one may obtain the change in scattering rate upon alloying. It is this approach that was adopted in analysis of the experimental data described here.

Once again, it should be emphasized that the values of Γ obtained are for small regions of the Fermi surface for which the resonance parameter has an extremum. This fact is in contrast with the analogous measurements obtained from de Haas–van Alphen Dingle temperature measurements. In de Haas–van Alphen measurements, the Dingle temperatures and hence the scattering rates are orbital averages. To obtain point-by-point scattering information from de Haas–van Alphen data, a fitting technique such as a symmetrized Fourier series[10] must be used. Although such an approach has proven to be highly successful in many materials,[10,11] it does introduce another possible source of error into the scattering rate measurements and might also fail to detect accurately rapid variations in the scattering rate. By comparison, the scattering rate may be obtained directly, on an almost point-by-point basis, from the experimental surface-state resonances through the application of a straightforward fit of theoretical calculations to the experimental data.

III. EXPERIMENT

A. Apparatus

The magnetic-field-induced surface-state measurements were made in a simple set of Helmholtz coils with a maximum field of 120 Oe, using a sample holder which allowed the rotation of the magnetic field through 360° about an axis perpendicular to the sample plane. The sample formed one end wall of a cylindrical microwave cavity. The change in sample surface impedance was detected by measurement of cavity Q using a conventional reflection type microwave spectrometer operating at 24.2 GHz. The spectrometer was similar in design to that employed by Koch and his co-workers and is amply described elsewhere.[5,8] The magnetic field was modulated at a frequency of 100 Hz to allow synchronous detection of the resulting signal and direct measurement of dR/dH. The work was conducted at liquid He temperatures (nominally 4.2 K).

B. Samples

The Cu sample used in the experiment was spark cut from a large single crystal boule. The starting crystal, nominally 99.999% pure, was obtained from Materials Research Corporation. After spark cutting, the Cu sample was annealed in a partial (4×10^{-4} mm Hg) oxygen atmosphere at 1000 °C for 10 days. The oxygen anneal was accomplished to improve the resistivity ratio by sequestering the residual impurities so as to render them ineffective as electron scatterers.

After annealing, the sample was lapped using 600 grit paper followed by aluminum oxide. A 2:1 solution of H_3PO_4 to water according to the recipe given by Tegart[12] was used to electropolish the samples. As reported by Doezema[5] the samples required several hours of polishing to obtain satisfacto-

ry results. Optimum polishing conditions were maintained by careful control of the cell voltage using a digital voltmeter and constant voltage power supply. After polishing, the samples were rinsed repeatedly with distilled water, dried with moisture-free air, and placed under vacuum.

In an effort to determine the quality of the oxygen annealed and polished pure copper sample, several cyclotron resonances were observed using a conventional electromagnet. The cyclotron resonance data was used to estimate the scattering rate for the samples. For these particular samples, $\omega\tau$ was found to be approximately equal to twenty (at $\omega = 24$ GHz). No attempt was made to measure the resistivity ratio, since past experiments have shown that such measurements are not reliable for surface-state work.

The Cu(Al) sample was prepared using the pure Cu sample described previously. A thin layer of aluminum was vacuum evaporated onto the polished, oxygen annealed pure copper sample. The aluminum was then diffused into the copper using a multistep annealing process. The multistep anneal was performed by heating the Al-coated Cu sample for 24 h at 300 °C in vacuum. The temperature was then raised to 600 °C for 316 h. The multistep anneal was undertaken to ensure a uniform Al concentration. After annealing the sample was electropolished to a predetermined depth to obtain a surface region with the desired Al concentration. Based on a diffusion theory calculation,[13] the resulting aluminum concentration is estimated to be between 10 and 50 ppm.

C. Scattering rate measurements and analysis in Cu and Cu(Al)

Scattering rate measurements were made for a variety of points on the Fermi surface in the pure Cu sample and Cu(Al) sample. The scattering rates were extracted by fitting the theoretical spectrum to experimentally measured data. In this technique, the scattering rate Γ is in essence a fitting parameter which relates the experimental resonance line shape to the theoretical resonance line-shape expression.[6]

To evaluate the theoretical expression for the resonance line shapes, it is necessary to know the value of $K_\perp$, the radius of curvature in the plane perpendicular to the magnetic-field direction, and the magnitude and direction of v_F the Fermi velocity. The needed values of $K_\perp$ were obtained using Halse's Fermi surface[14] for Cu. One can also obtain the direction of the normal to the Fermi surface (i.e., direction of v_F) from Halse's Cu Fermi surface. The magnitude of the Fermi velocity was obtained from surface-state measurements by Doezema.[8]

The evaluation of the experimental resonance

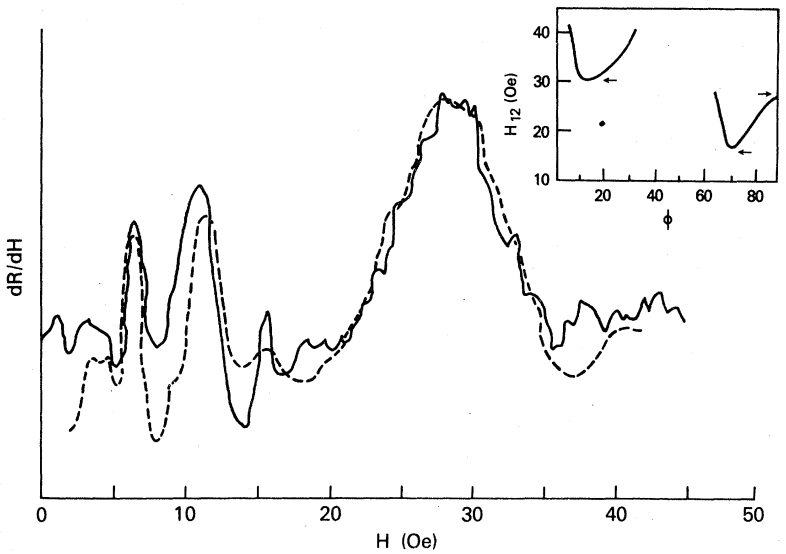

FIG. 2. Comparison of the experimental resonance spectrum (solid line) in Cu with that predicted by theory (dashed line) for H parallel to $\langle 100 \rangle$ and j_{rf} parallel to H. Inset depicts predicted minima and maxima in plot of resonant field value for transitions between first and second surface-state energy levels. The angle ϕ is measured from the $\langle 100 \rangle$ axis with respect to the center of the zone.

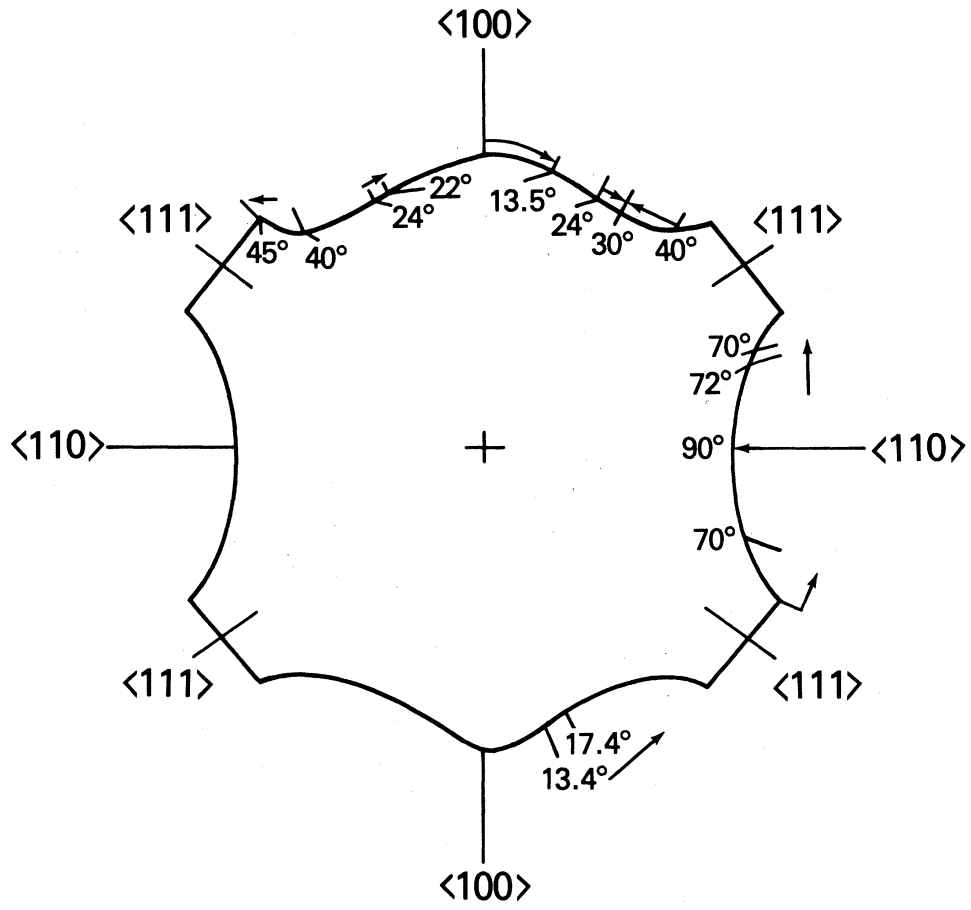

FIG. 3. Fermi-surface regions in the (110) plane of Cu that give rise to surface-state resonances (Ref. 8). Angular measurements are made from the ⟨100⟩ with respect to the center of the zone. The arrows denote the approximate region of the Fermi surface contributing to the signal.

spectra was carried out as follows. A set of theoretical curves was generated for a range of Γ values ($\Gamma^* = 0.5$ to 0.1). A graphing routine was used to plot the predicted spectrum for comparison with the actual observed experimental resonance spectrum. The Γ^* value selected was the one giving rise to the best agreement between prediction and experiment as shown in Fig. 2.

To identify the location on the Fermi surface giving rise to the observed resonances, the technique adopted by Doezema[8] was employed. Theoretical plots of the resonant magnetic field, as given in Eq. (1), corresponding to transitions between the first and second surface-state energy levels H_{12} were developed as a function of Fermi-surface location and magnetic field orientation. Local minima and maxima in the plot of H_{12} were then used to predict regions of the Fermi surface which would give rise to the observed resonances. The inset in Fig. 2 depicts one such calculation. The arrows indicate points that correspond to the Fermi-surface regions having local resonant magnetic field minima and maxima. The various regions of the Fermi surface from which signals can be observed are shown in Fig. 3.

It should be pointed out that for some magnetic field orientations, signals may be observed simultaneously from several regions of the Fermi surface. The result is a complex spectrum consisting of multiple overlapping spectra. This situation is analogous to what occurs in the de Haas–van Alphen effect when signals from more than one extremal area are present. For surface states, it is possible to selectively excite various regions of the Fermi surface by careful choice of magnetic and microwave electric field orientation. A total of eleven magnetic and two electric field orientations were used to obtain the desired surface-state resonances.

D. Experimental Results

Scattering rates were measured in the pure Cu and Cu(Al) samples. The dramatic change in shape of the resonance spectrum generally seen upon alloying is shown in Fig. 4. Shown are resonance spectra from the (110) sample plane of pure Cu and Cu(Al). A series of twenty-six such spectra were recorded and analyzed for scattering rates for Cu and Cu(Al). In addition, the change in scattering rate upon alloying $\Delta\Gamma^*$ is also given as is the point on the Fermi surface from which the signals originate. Figure 5(a) shows the change in scattering rate as a function of Fermi-surface location. The angle ϕ is taken with respect to the [100] axis and the center of the zone.

The observed anisotropy is also consistent with measurements obtained by Coleridge and Templeton[15,16] using the de Haas–van Alphen effect. They measured the variation in the Dingle temperature χ over the Cu Fermi surface in a number of Cu(Al) alloys. The Dingle temperatures are directly related to the scattering time τ through the relation

$$\chi = h/k_B\tau \,, \tag{10}$$

where k_B is Boltzmann's constant. Using this relationship, one may obtain the variation in total scattering rate S which should be proportional to $\Delta\Gamma^*$. Given the relatively large combined errors for the lowest scattering rate points (approximately 30–50%) we see that the two sets of results are in excellent agreement regarding the anisotropy while the difference in scale factor arises from different levels of impurity content.

IV. DISCUSSION

A. Scattering anisotropy

The anisotropy of the electron impurity scattering is evidenced by the data in Fig. 5(a). The scattering is highest for electron states near the ⟨111⟩ neck and ⟨100⟩ region. It is lowest for regions around $\phi = 20°$ to 30° and the ⟨110⟩ point. There is also a smooth variation of the scattering rate evident as one moves from the ⟨100⟩ direction towards the ⟨111⟩ and thence to the ⟨110⟩ directions. The measured scattering rate is found to vary by a factor of 3.3 over the Fermi surface.

As is well known, the scattering rate for any particular state, k, on the Fermi surface is proportional to $\Sigma_k |\langle k^* | V | k \rangle|^2$, where k^* is the initial state, k the final state, and V the perturbing potential. Thus the scattering anisotropy will depend on both the detailed symmetry of the scattering potential and the variation of the specific nature of the electron wave functions over the Fermi surface. In copper this variation is quite pronounced as shown by augmented-plane-wave (APW) calculations in that the relative amounts of s, p, and d components in the wave functions vary sharply as a function of position on the Fermi surface. In particular, the

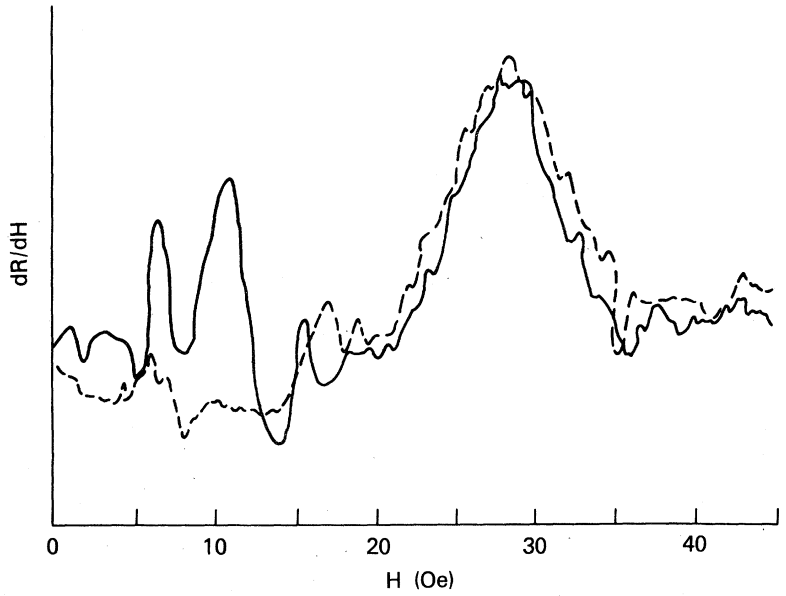

FIG. 4. Comparison of magnetic-field-induced surface-state resonances in Cu (solid line) and Cu(Al) (dashed line). H is parallel to ⟨100⟩ and j_{rf} is parallel to ⟨100⟩.

values of the fraction of *s*, *p*, and *d* state present in the ⟨110⟩ plane of copper are shown in Fig. 5(b).

An interesting observation may be made by comparing the variation in *s*, *p*, and *d* wave components of the Cu electron wave function over the Fermi surface with the variation in scattering rate. Figure 5(b) is a plot of the amplitude of the *s*, *p*, and *d* wave components of the Cu electron wave functions obtained from augmented-plane-wave calculations[17,18] versus the angle ϕ. Figure 5(a) is a plot of the change in scattering rate $\Delta\Gamma^*$ versus ϕ. As is clearly seen, the correlation between the *p*-state fraction of the wave function and the scattering rate is very close. Since impurity scattering is known to be, basically, large-angle scattering and since the band calculations suggest that the copper Fermi surface as a whole contains roughly comparable fractions of *p* and *d* wave functions and somewhat lesser amounts of *s* wave functions, it can be concluded that the scattering potential introduced in Cu by Al connects primarily the *p* states.

It should be noted that this could not be concluded under other physical conditions. If, for example, there were a preponderance of *d*-like states on the Fermi surface compared to *p*-like states, then we could not draw this same conclusion. In this case we might also explain our high *p*-state scattering rate by a scattering potential that mixed *p* and *d* states. The individual *p* states would be more highly scattered because they would have a high density of final *d* states to be scattered into, whereas the individual *d* state would have a low density of final *p* states to be scattered into and thus a low scattering rate. Note also that if impurity scattering was dominated by low-angle scattering, which is not the case, then our results could again be explained by a scattering potential that connected *p* states with *p* states and *p* states with say *d* states. The *p*-*d* scattering process might then not occur, however, because the *p* and *d* states could be located at different points on the Fermi surface which could not be bridged by small angle scattering.

Our conclusion that the Al scattering potential links primarily initial and final *p* states in the scattering process is supported in a semiquantitative way by the relative magnitudes of the anisotropies of the scattering rate and the *p* component of the wave functions. In the extreme approximation where one assumes that *only* the *p* component of the wave functions are scattered and that this scattering is *totally* independent of angle then one predicts a scattering rate proportional to the square of the *p*-state component of the electron wave function.

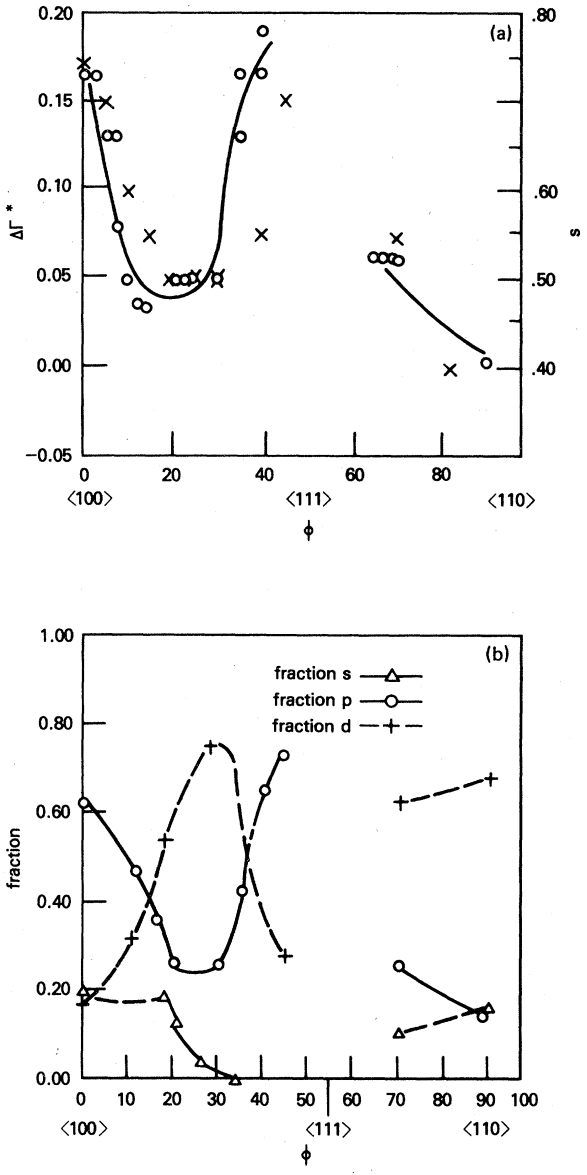

FIG. 5. (a) Comparison of $\Delta\Gamma^*$, as a function of Fermi-surface location, to deduced variation of total scattering rate, *S*, from de Haas–van Alphen studies of Cu(Al). ○ this study; × Coleridge and Templeton (Refs. 15 and 16). (b). The fraction of *s*, *p*, and *d* state in the Cu electron wave functions vs Fermi-surface location ϕ in the (110) plane measured with respect to the ⟨100⟩ axis from the center of the zone.

Within experimental error and the probable precision of our assumptions, this is precisely what is seen in comparing the scattering anisotropy data and *p*-state anisotropy shown in Fig. 5. For exam-

TABLE I. Γ^* results for the (110) plane in Cu and Cu(Al) versus θ, the angle the magnetic field makes with the $\langle 110 \rangle$ axis. The angle ϕ is measured from the $\langle 100 \rangle$ direction and locates the contributing electrons. The angle $\Delta\phi$ is a measure of the strip width over which there are significant contributions to Γ^*.

θ (deg)	ϕ (deg)	$\Delta\phi$ (deg)	Γ^* (Cu)	Γ^* [Cu(Al)]	$\Delta\Gamma^*$
90	90	80 – 90	0.25	0.25	0.0
	70	66.5 – 75	0.14	0.20	0.06
	13	8.5 – 23.7	0.17	0.20	0.03
80	69	66.5 – 75	0.14	0.20	0.06
	70	66.5 – 75	0.14	0.20	0.03
75	67.5	66.5 – 75	0.14		
	25	24.7 – 40	0.20	0.25	0.05
	10	6.5 – 20	0.20	0.25	0.05
70	27.5	25 – 35	0.20	0.25	0.05
	10	6.5 – 20	0.20	0.25	0.05
60	25	25 – 38	0.20	0.25	0.05
	7.5	4 – 20	0.20	0.25	0.05
50	72.5	69 – 76	0.14	0.20	0.06
	67.5	65 – 72.5	0.14	0.20	0.06
	27.5	27.5 – 40.5	0.20	0.25	0.05
	7.5	2.5 – 22.5	0.20	0.33	0.13
40	72.5	69 – 76	0.14	0.20	0.06
	65	64.5 – 66		0.20	
	30	29.5 – 45	0.20	0.25	0.05
	7.5	1.6 – 15	0.20	0.33	0.13
30	40	38 – 44.5	0.17	0.33	0.17
	35	34.5 – 39	0.17	0.33	0.17
	24	18.5 – 34.5	0.20	0.25	0.05
	20	10.7 – 34.5	0.20		
	6.5	1.2 – 12.5	0.25	0.33	0.08
20	40	38 – 42.5	0.14	0.33	0.19
	35	30 – 41.5	0.20	0.33	0.13
	24.5	14 – 30	0.20	0.25	0.05
	21.5	10.5 – 38	0.20	0.25	0.05
	5.5	0 – 14	0.20	0.33	0.13
10	40	30 – 41.5	0.14	0.33	0.19
	40	30 – 41.5	0.14	0.33	0.19
	23	10 – 30	0.20	0.25	0.05
	22.5	10 – 30	0.20	0.25	0.05
	3.0	0 – 10	0.17	0.33	0.17
0	40	27.5 – 42.5	0.14	0.33	0.19
	22.5	10 – 27.5	0.20	0.25	0.05
	0	0 – 7.5	0.17	0.33	0.17

ple, between the maximum at the ⟨100⟩ axis and the minimum at $\phi \simeq 30°$ the p-state wave function falls by a factor of approximately 0.45, and thus, the square by a factor of roughly 0.20. Between the same two points the scattering falls by a factor of approximately 0.30, in good semiquantitative agreement.

It is of interest to note that Al has primarily p electronic structure and according to our results primarily scatters p-state electrons at the Fermi surface. This correlation is not *necessarily* what one would expect to obtain from a straightforward application of an APW band-structure calculation-type approach to electron scattering.[18] We intend to return to this question in more detail in a future publication. For the moment, suffice to say that we believe that surface-state resonance experiments may provide an important and sensitive test of both the local perturbing potential of impurities in metals and the detailed numerical procedures used in band structure calculations.

In conclusion, we have used magnetic-field-induced surface states to study the change in scattering rate upon alloying of Cu with Al. We have found a close correlation between the change in electron scattering rate and p-wave content of the electrons on the Fermi surface.

ACKNOWLEDGMENTS

We would like to express our gratitude to the staff of the Metal Physics Branch, Naval Research Laboratory, Washington, D.C. for their assistance in this work. In particular, we are indepted to D. A. Papaconstantopoulos and his associates for providing wave-function data and advice. We also wish to acknowledge the valuable assistance and advice provided by Dr. R. Meussner regarding the metallurgical aspects of the program.

[1]R. E. Prange and T. W. Nee, Phys. Rev. 168, 779 (1968).
[2]T. W. Nee, J. F. Koch, and R. E. Prange, Phys. Rev. 174, 758 (1968).
[3]J. F. Koch, in *Electrons in Metals,* edited by J. F. Cochran and R. R. Haering, Vol. I of *Solid State Physics* (The Simon Fraser University Lectures) (Gordon and Breach, New York, 1968).
[4]M. S. Khaikan, Adv. Phys. 18, 1 (1969).
[5]R. E. Doezema and J. F. Koch, Phys. Rev. B 6, 2071 (1972).
[6]T. Wegehaupt and R. E. Doezema, Phys. Rev. B 16, 2515 (1977).
[7]*Handbook of Mathematical Function,* U. S. Natl. Bur. Stand. (Appl. Math. Ser. No. 55), edited by M. Abramowitz and J. A. Stegun (U. S. GPO, Washington, D. C., 1964).
[8]R. E. Doezema and J. F. Koch, Phys. Rev. B 5, 3866 (1972).
[9]J. F. Koch and J. D. Jensen, Phys. Rev. 184, 643 (1969).
[10]D. L. Lowndes, K. M. Miller, R. G. Poulsen, and M. Springford, Proc. R. Soc. London, Ser. A 331, 497 (1973).
[11]R. G. Poulsen, D. L. Randles, and M. Springford, J. Phys. F 4, 981 (1974).
[12]W. J. Tegart, *The Electrolytic and Chemical Polishing of Metals in Research and Industry* (Pergamon, London, 1959).
[13]W. Jost, *Diffusion* (Academic, New York, 1960).
[14]M. R. Halse, Philos. Trans. Ser. A 265, 507 (1969).
[15]P. T. Coleridge and I. M. Templeton, Can. J. Phys. 49, 2449 (1971).
[16]P. T. Coleridge, J. Phys. F 2, 1016 (1972).
[17]D. A. Papaconstantopoulos, L. L. Boyer, B. M. Klein, A. R. Williams, V. L. Moruzzi, and J. F. Janak, Phys. Rev. B 15, 4221 (1977).
[18]D. A. Papaconstantopoulos (private communication).